



ELSEVIER

PHYSICA



Chemical trends of superconducting properties in pyrochlore oxides

Zenji Hiroi,^{a,*} Jun-Ichi Yamaura,^a Shigeki Yonezawa,^a Hisatomo Harima^b

^aInstitute for Solid State Physics, University of Tokyo, Kashiwa, Chiba 277-8581, Japan

^bDepartment of Physics, Kobe University, Kobe, Hyogo 657-8501, Japan

Elsevier use only: Received date here; revised date here; accepted date here

Abstract

Chemical trends of fundamental superconducting parameters and normal-state properties are described for a family of pyrochlore oxide superconductors. Particularly, the change of T_c from 1.0 K for α -pyrochlore $\text{Cd}_2\text{Re}_2\text{O}_7$ to 3.3 K ($A = \text{Cs}$), 6.3 K (Rb), and 9.6 K (K) for β -pyrochlore AOs_2O_6 is discussed on the basis of the conventional BCS scheme. Enhanced T_c and anomalous features observed for KOs_2O_6 are ascribed to low-energy phonons probably coming from the rattling of the K cations.

© 2001 Elsevier Science. All rights reserved

Keywords: superconductivity; rattling; pyrochlore oxide; specific heat; resistivity

1. Introduction

Twenty years have already passed after the discovery of Cu-based oxide superconductors in 1986 [1], and many related superconductors have been synthesized successfully. Consequently, it is getting more and more difficult to find a new one. On the other hand, the search for non-Cu-based oxide superconductors has been extended during the last decade, which mainly aims to understand the role of electron correlations in the mechanism of superconductivity or to search for a novel pairing mechanism, hopefully to reach a higher T_c .

An interesting example is a family of pyrochlore oxide superconductors. The first discovered is α -pyrochlore $\text{Cd}_2\text{Re}_2\text{O}_7$ with $T_c = 1.0$ K [2] and the second β -pyrochlore AOs_2O_6 with $T_c = 3.3, 6.3,$ and 9.6 K for $A = \text{Cs}$ [3], Rb [4-6], and K [7], respectively. They crystallize in the cubic pyrochlore structure of the same space group of $Fd-3m$ [8] and commonly possess a 3D skeleton made of ReO_6 or OsO_6 octahedra, as illustrated in Fig. 1. The difference between the two types comes from the fact that the O' atom

at the $8b$ site in the α -pyrochlore $\text{Cd}_2\text{Re}_2\text{O}_6\text{O}'$ is replaced by the A atom in the β -pyrochlore AOs_2O_6 [9, 10]. Moreover, the Cd $16d$ site in the former is vacant in the latter. This means, in other words, that a relatively large CdO_4 tetrahedral unit is replaced by a single A atom which must suffer a large size mismatch and can rattle in an oversized atomic cage. It was pointed out that this mismatch causes a peculiar anharmonic vibration, particularly for the smallest K atom [10-12].

The electronic structures of α - $\text{Cd}_2\text{Re}_2\text{O}_7$ and β - AOs_2O_6 have been calculated by first-principle density-functional methods, which reveal that a metallic conduction occurs in the (Re, Os)-O network [12-16]: electronic states near the Fermi level originate from transition metal 5d and O 2p orbitals. Although the overall shape of the density of state (DOS) is similar for the two compounds, the difference in band filling results in different properties; Re^{5+} for α - $\text{Cd}_2\text{Re}_2\text{O}_7$ has two 5d electrons, while $\text{Os}^{5.5+}$ for β - AOs_2O_6 has two and a half. It is to be noted that a related α -pyrochlore $\text{Cd}_2\text{Os}_2\text{O}_7$ with Os^{5+} ($5d^3$) exhibits a metal-to-insulator transition at 230 K [17, 18].

The mechanism of superconductivity for the pyrochlore oxides has been studied extensively so far. Most of data

* Corresponding author. Tel.: +81-47136-3445; fax: +81-47136-3446; e-mail: hiroi@issp.u-tokyo.ac.jp.

obtained for $\text{Cd}_2\text{Re}_2\text{O}_7$ have revealed that it is a weak-coupling BCS-type superconductor [19, 20]. Experimental efforts to elucidate the nature of the superconductivity of the β -pyrochlores are in progress [11, 21-34]. Interestingly to be compared with $\text{Cd}_2\text{Re}_2\text{O}_7$, there are several findings which suggest unconventional features for AOs_2O_6 . For example, resistivity exhibits an anomalous concave-downward curvature, indicating an unusual scattering process involved in the normal state [7]. Moreover, NMR experiments by Arai *et al.* showed a tiny coherence peak in the relaxation rate below T_c for RbOs_2O_6 , while no peaks were found for KOs_2O_6 [24]. This is in strong contrast to the result for $\text{Cd}_2\text{Re}_2\text{O}_7$ in which a huge coherence peak was detected [20]. In this paper, we consider systematic variations of various properties over the series, especially of T_c , in order to get meaningful insights on the mechanism of superconductivity and the source of the unconventional properties. The results of band structure calculations are also presented to understand the chemical trends.

2. Experimental

Samples were prepared as reported previously [3, 4, 7, 9]. Single crystals of 1 mm size were obtained for $\text{Cd}_2\text{Re}_2\text{O}_7$ and KOs_2O_6 , while only polycrystalline samples were available for CsOs_2O_6 and RbOs_2O_6 , which caused a certain ambiguity for data obtained. The electrical resistivity and specific heat were measured in a Quantum Design physical property measurement system.

3. Results and discussion

3.1. Specific heat

Figure 2 compares specific heat data for the 4 compounds [11, 19, 22]. The superconducting transition is

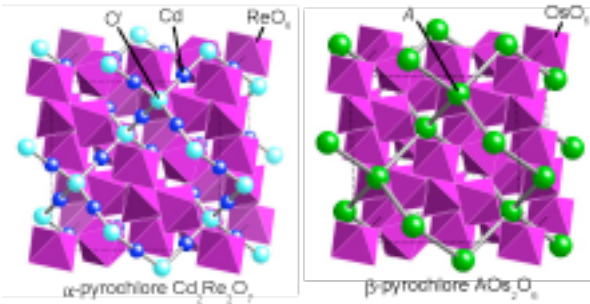


Fig. 1. Comparison of crystal structures between α -pyrochlore $\text{Cd}_2\text{Re}_2\text{O}_7$ (left) and β -pyrochlore AOs_2O_6 (right). They possess the same skeleton made of ReO_6 or OsO_6 . The difference comes from the fact that the O' atom in the former is replaced by the A atom in the latter with the nearby Cd sites vacant.

sharp for single crystals of $\text{Cd}_2\text{Re}_2\text{O}_7$ and KOs_2O_6 , while is relatively broad for polycrystalline samples of CsOs_2O_6 and RbOs_2O_6 . The magnitude of the jump at T_c , $\Delta C/\gamma T_c$, is 1.15 and 2.83 for $\text{Cd}_2\text{Re}_2\text{O}_7$ and KOs_2O_6 , respectively, indicating that the latter is an extremely strong-coupling superconductor.

It is to be noted in Fig. 2 that the magnitude of specific heat above T_c is very different among the 4 compounds. Compared at 10 K, for example, it is a factor of 8 larger for KOs_2O_6 than $\text{Cd}_2\text{Re}_2\text{O}_7$. This must be due to the difference in lattice contributions, not electronic ones, and is surprising because the lattice specific heat of such an identical or closely related structures should be similar. In the case of $\text{Cd}_2\text{Re}_2\text{O}_7$, the electronic and lattice parts could be reasonably separated as $C = \gamma T + \beta T^3$, assuming a Debye-type phonon at low temperature: $\gamma = 30.2 \text{ mJ K}^{-2} \text{ mol}^{-1}$ and $\beta = 0.222 \text{ mJ K}^{-4} \text{ mol}^{-1}$ that yields the Debye temperature $\Theta_D = 460 \text{ K}$ [19]. In contrast, it was found that the temperature dependence of the normal-state specific heat for the Cs and Rb compounds is unusually expressed as $C = \gamma T + \beta T^5$ in a wide temperature range between 0.5 and 7 K [11]. Very recently, we found the same T^5 dependence for a single crystalline KOs_2O_6 [35].

Thus, in the β pyrochlores, usual Debye phonons may be masked by other types of low-energy phonons or other excitations. Possibly related to this, high-temperature specific heat is greatly enhanced due to the contribution from Einstein-like phonons. By fitting the data, Einstein temperature Θ_E was obtained as $\Theta_E = 70, 61, \text{ and } 40 \text{ K}$, for $A = \text{Cs, Rb, and K}$, respectively [11]. These must correspond to the specific frequency of the rattling motion of the alkali ions. The second anomaly observed at $T_p = 7.5 \text{ K}$ for the specific heat of the K compound was reported in our previous paper, which may indicate a structural

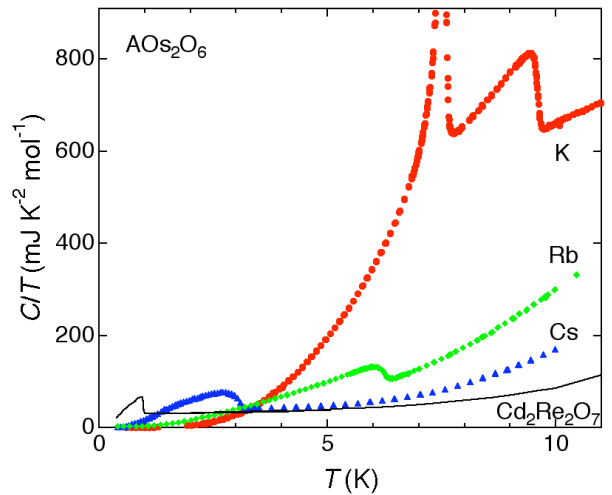


Fig. 2. Specific heat divided by temperature for $\text{Cd}_2\text{Re}_2\text{O}_7$ and AOs_2O_6 . The data for $\text{Cd}_2\text{Re}_2\text{O}_7$ and KOs_2O_6 were obtained from single crystals and those for CsOs_2O_6 and RbOs_2O_6 from polycrystalline samples.

transition associated with rattling K cations [21, 22]. The γ value and the magnitude of the jump at T_c are given in Table 2.

3.2. Resistivity

Figure 3 compares the temperature dependence of resistivity. Polycrystalline Cs and Rb samples exhibit a concave-downward resistivity at high temperature, followed by T^2 behavior at low temperature below a certain temperature T^* of ~ 20 K and ~ 15 K, respectively. In contrast, the resistivity of the polycrystalline K sample shows a concave-downward curvature in a whole temperature range above T_c . Essentially the same temperature dependence is observed for a single crystalline K sample [22]. Figure 3(c) shows resistivity data measured at a magnetic field of 140 kOe for the single crystal of KOs_2O_6 , where the T_c is reduced to 5.2 K. Remarkably, a sudden drop in the normal-state resistivity is observed at $T_p = 7.5$ K, where the specific heat exhibits a sharp peak (Fig. 2). Moreover, the temperature dependence below T_p is proportional to T^2 . These changes of the normal-state resistivity must imply that the scattering mechanism of carriers is substantially changed at T_p . Consequently, commonly observed in the resistivity of the β pyrochlores is the change from high-temperature concave-downward to low-temperature T^2 behavior, which takes place as a crossover at T^* for Cs and Rb, while as a phase transition at T_p for K. The former temperature dependence suggests a strong electron-phonon interaction possibly ascribed to the rattling of A cations, while the latter may indicate that electron-electron scattering dominates at low temperature, as suggested also by recent thermal conductivity measurements [34]. From a structural point of view, this implies that the rattling motion is frozen below T^* for Cs and Rb, while it undergoes a cooperative phenomenon at T_p for K due to a finite interaction between the rattlers [22].

In contrast, the resistivity of α -pyrochlore $\text{Cd}_2\text{Re}_2\text{O}_7$ exhibits more conventional features at high temperature, as shown in Fig. 3(a). Moreover, T^3 behavior, not T^2 , is observed at low temperature below 27 K, as shown in Fig. 3(c), which may be due to scattering by phonons on the cage.

One more remark on the single crystal of KOs_2O_6 is its small residual resistivity, $\rho_0 \sim 1 \mu\Omega \text{ cm}$, which was estimated by extrapolating the T^2 dependence to $T = 0$. Since the room temperature resistivity is $\sim 300 \mu\Omega \text{ cm}$, the residual resistivity ratio (RRR) reaches 300, which is unusually large for transition metal oxides. The RRR of the $\text{Cd}_2\text{Re}_2\text{O}_7$ crystal shown in Fig. 3 is only 30. The residual resistivity is generally given as

$$\rho_0 = \frac{\hbar(3\pi^2)^3}{e^2 \ell n^{-2/3}},$$

where ℓ and n are the mean-free-path and density of carriers, respectively. Since the carrier density has not yet been determined experimentally, we calculated it from the band structure calculations mentioned later; $n = 2.8 \times 10^{21} \text{ cm}^{-3}$.

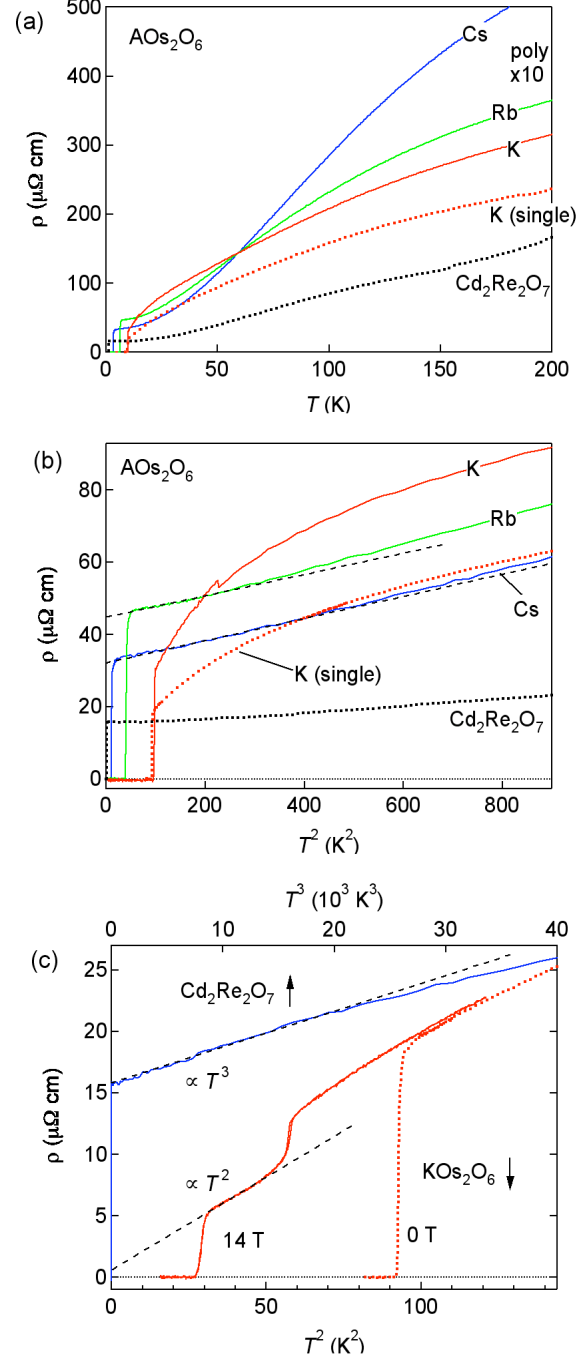


Fig. 3. Resistivity for polycrystalline AO_3O_6 (solid lines) and single-crystalline KOs_2O_6 and $\text{Cd}_2\text{Re}_2\text{O}_7$ (dotted lines) plotted as a function of T in a wide temperature range (a) and as a function of T^2 at low temperature below 30 K (b). In (c), resistivity of the single-crystalline KOs_2O_6 measured at a magnetic field of 14 T is plotted against T^2 (lower axis), and the resistivity of $\text{Cd}_2\text{Re}_2\text{O}_7$ is plotted against T^3 (upper axis). Broken straight lines are the guides to the eye.

Then, we obtain a large mean-free-path of 640 nm, which is comparable to the value of the most cleanest crystal of Sr_2RuO_4 [36]. Since the superconducting coherence length ξ of KOs_2O_6 is 3.3 nm, it is definitely in the regime of ultra clean limit.

Table 1

Summary of superconducting and normal-state properties for α -pyrochlore $\text{Cd}_2\text{Re}_2\text{O}_7$ and β -pyrochlore AOs_2O_6 of $A = \text{Cs, Rb, K}$

	$\text{Cd}_2\text{Re}_2\text{O}_7$	CsOs_2O_6	RbOs_2O_6	KOs_2O_6
T_c (K)	1.0	3.3	6.3	9.6
$\mu_0 H_{c2}$ (T)	0.29	~ 3.3	~ 5.5	30.6
ξ (nm)	34	~ 10	~ 7.8	3.3
λ (nm)	460	400	234	270
GL parameter	14	~ 40	~ 30	82
$\Delta C/\gamma T_c$	1.15	~ 1	~ 1	2.87
γ_{exp} ($\text{mJ K}^{-2} \text{mol}^{-1}$)	30.2	~ 40	~ 40	71
γ_{band} ($\text{mJ K}^{-2} \text{mol}^{-1}$)	11.5	11.0	10.2	9.6

Table 2

Summary of structural parameters for α -pyrochlore $\text{Cd}_2\text{Re}_2\text{O}_7$ and β -pyrochlore AOs_2O_6 of $A = \text{Cs, Rb, K}$

	$\text{Cd}_2\text{Re}_2\text{O}_7$	CsOs_2O_6	RbOs_2O_6	KOs_2O_6
a (nm)	1.02232	1.01525	1.01176	1.01065
x (O) ^a	0.3137	0.3146	0.3180	0.3160
U_{iso} (10^{-4}nm^2) ^b	1.1	2.5	4.3	7.7
Ionic radius (nm)	0.095	0.167	0.152	0.138
Θ_E (K)	-	70	61	~ 40

^aAtomic coordinate of 48f oxygen; (x 0 0).

^bAtomic displacement parameter for Cd or A.

3.3. Chemical trends

Figure 4 summarizes the evolution of several experimental parameters, γ , $\Delta C/\gamma T_c$, H_{c2} , Θ_E and U_{iso} , as a function of T_c . The γ value is much larger in each case than the bare electronic value obtained from band structure calculations, which decreases slightly with increasing T_c , as reported previously [12, 16]. The enhancement factor $\gamma_{\text{exp}}/\gamma_{\text{band}}$ is 2.6 (Re), 3.6 (Cs), 3.9 (Rb), and 7.4 (K), which give large renormalization factors λ in $\gamma_{\text{exp}}/\gamma_{\text{band}} = 1 + \lambda$. The relation between γ and T_c is discussed later. To be stressed here is the exceptionally large enhancement for K. This is also the case for other parameters, $\Delta C/\gamma T_c$ and H_{c2} , suggesting some additional effect must be present for K. The H_p in Fig. 4(c) is the paramagnetic limit of the upper critical field simply calculated as $H_p = 1.85T_c$. The H_{c2} value is lower than H_p except for the case of K. However, it was pointed out for K, by taking account of experimental normal-state magnetic susceptibility, that an actual H_p is approximately 30 T, close to the experimental value [32, 34].

On the other hand, the structural parameters change systematically. The Einstein temperature decreases and the atomic displacement parameter of the A cations increases from Cs to K [9, 10]. This implies that the characteristic energy of rattling is lowered toward K with decreasing the size of the rattler and thus increasing the available space in a cage. Several structural parameters are listed in Table 2.

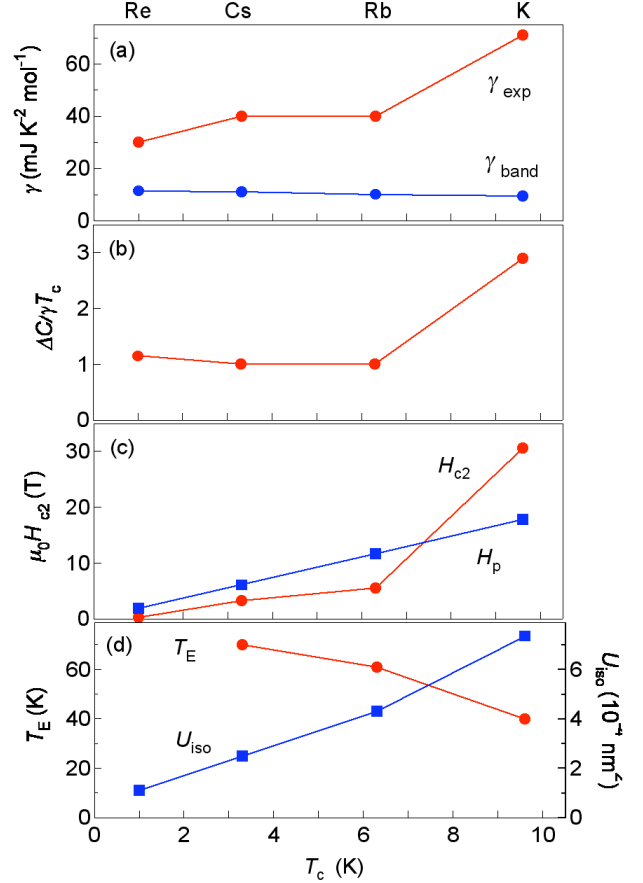


Fig. 4. Evolution of Sommerfeld coefficient γ (a), jump in specific heat at T_c , $\Delta C/\gamma T_c$ (b), upper critical field H_{c2} (c), and Einstein temperature Θ_E and atomic displacement parameter U_{iso} (d) as a function of T_c .

3.4. Bandstructure calculations

Electronic bandstructure calculations were carried out for α -pyrochlores $\text{Cd}_2\text{Re}_2\text{O}_7$ and $\text{Cd}_2\text{Os}_2\text{O}_7$ as well as for β -pyrochlores AOs_2O_6 . As reported already by other groups [12-16], these 5d pyrochlore oxides possess a strongly hybridized band made of Re/Os 5d and O 2p states near the Fermi level, which is a manifold of 12 bands with a total bandwidth of ~ 3 eV. Because of the large bandwidth, they may not be classified as strongly correlated electron systems in the ordinary sense. As shown in Fig. 5, the profile of the density-of-states (DOS) is similar among

them, exhibiting many sharp peaks due to a large degeneracy coming from the high symmetry of the pyrochlore structure. The major difference between α and β pyrochlores comes from the fact that there is a finite contribution from the Cd 4d states to the E_F state in α , while almost nothing from alkali metals in β .

The great variation of physical properties arises from band filling; $5d^2$, $5d^{2.5}$ and $5d^3$ for $\text{Cd}_2\text{Re}_2\text{O}_7$, AOs_2O_6 , and $\text{Cd}_2\text{Os}_2\text{O}_7$. As shown in Fig. 5, the E_F is located near a valley in $\text{Cd}_2\text{Re}_2\text{O}_7$, which results in a small Fermi surface around the zone center and a low carrier density [13]. In contrast, the E_F happens to lie close to a sharp peak at the middle of the manifold for $\text{Cd}_2\text{Os}_2\text{O}_7$ [14], which causes a certain magnetic instability leading to a metal-to-insulator transition (the low-temperature phase is not completely insulating, because of a part of the Fermi surface may

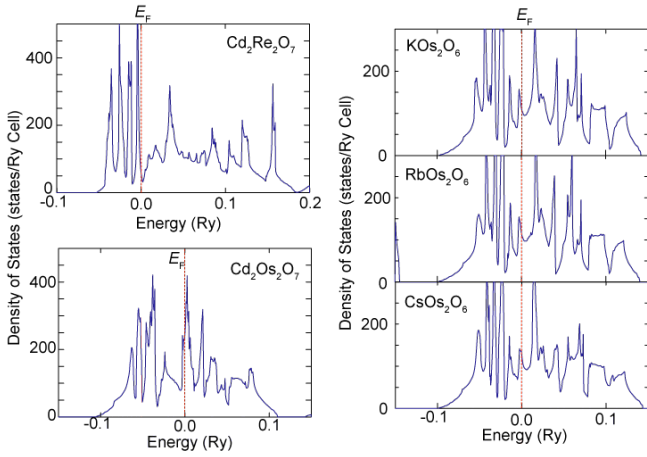


Fig. 5. Density of states near the Fermi level of the pyrochlore oxides.

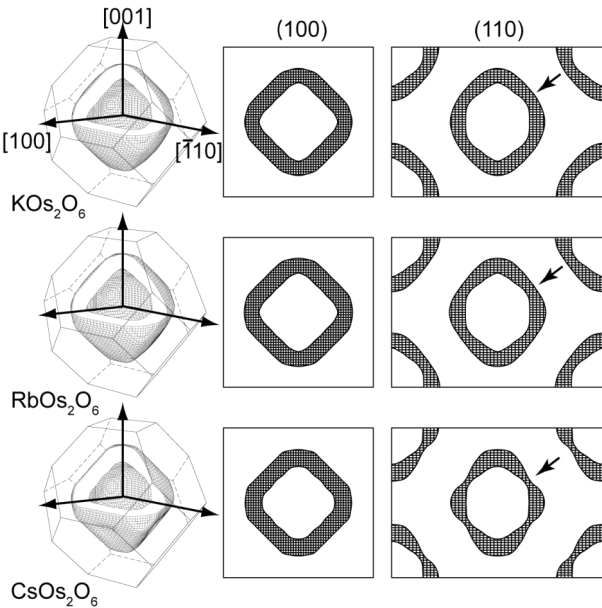


Fig. 6. Calculated Fermi surfaces for the three members of the β pyrochlores. (100) and (110) cross sections are also shown.

survive). Thus, electron correlations may play a role in $\text{Cd}_2\text{Os}_2\text{O}_7$ to some extent [18]. In contrast, β -pyrochlore AOs_2O_6 possesses a moderately large DOS between the two α pyrochlores, where one expects a moderately large electron correlations.

The evolution of the bandstructure for the β pyrochlores from Cs to K is unexpectedly subtle, as reported in previous study [12, 15, 16]. Because almost no contributions to the bandstructure arise from alkali metals in β , the bandstructure is roughly scaled to the lattice constant: the smaller the lattice, where larger hybridizations occur, the smaller the calculated DOS, as shown in Fig. 4. This is apparently different from the experimental observations. In order to explain the observed large enhancement of γ toward K, an additional effect must be taken into account. Here we point out that a significant change occurs for a pair of Fermi sheets over the series of compounds.

The calculated Fermi surface of β - AOs_2O_6 consists of a pair of closed sheets around the zone center and a hole-like sheet near the zone boundary. As shown in Fig. 6, the former Fermi surface possesses a characteristic shape: each sheet is not spherical but close to an octahedron with flat surfaces, suggesting an electronic instability due to Fermi surface nesting. Moreover, the two sheets are nearly homothetic. There is an interesting theoretical argument that such disconnected Fermi surfaces would suppress pair breaking and thus lead to an enhanced T_c [37]. It is apparent from the cross section perpendicular to the [110] direction, as illustrated in Fig. 6, that the two sheets are nearly parallel to each other for K, while the outer sheet dents toward the inner sheet for Cs. Thus, nesting tendency must be enhanced from Cs to K. It is plausible that this nesting feature plays some role in the mass enhancement and also the superconductivity in the β pyrochlores.

3.5. Normal-state properties

Here we consider electron correlations and mass enhancements for the pyrochlore oxides. Figure 7 displays a Kadowaki-Woods plot where many metallic compounds are mapped in the space of the coefficient A of the T^2 term in resistivity and the Sommerfeld coefficient γ [38, 39]. In the case of KOs_2O_6 , the A value of $0.143 \mu\Omega \text{ cm K}^{-2}$ from Fig. 3(c) and the γ value of $71 \text{ mJ K}^{-2} \text{ mol}^{-1}$ yield $A/\gamma^2 = 2.8 \times 10^{-5}$, close to the universal value of 10^{-5} , which implies that KOs_2O_6 is akin to the strongly correlated system. For Cs and Rb, we could not determine the value, because the A value must be overestimated owing to the polycrystalline nature.

Another important parameter for the strongly correlated system is the Wilson ratio R_W that is χ_s/γ . In the case of $\text{Cd}_2\text{Re}_2\text{O}_7$, the magnetic susceptibility measurements gave $\chi_0 = 4.7 \times 10^{-4} \text{ emu/mol}$, which should include an orbital contribution of $3.2 \times 10^{-4} \text{ emu/mol}$, as determined from Cd NMR measurements [40]. Thus, the spin susceptibility $\chi_s = 1.5 \times 10^{-4} \text{ emu/mol}$, which yields $R_W = 0.34$. This small R_W

may be consistent with the absence of T^2 term in resistivity. On the other hand, the χ_0 value of the present single crystalline KOs_2O_6 was $\chi_0 = 4.6 \times 10^{-4}$ emu/mol, similar as for $\text{Cd}_2\text{Re}_2\text{O}_7$. Assuming the same orbital contribution as for $\text{Cd}_2\text{Re}_2\text{O}_7$, $\chi_s = 1.4 \times 10^{-4}$ emu/mol, which gives a small R_W of 0.14. Such a small values of R_W generally implies strong electron-phonon interactions that must enhance only γ and less importance of conventional electron correlations.

In the case of Cs and Rb, the χ_0 value is similar to that of K, although there is an uncertainty from the sample quality. The R_W value may be also small, ~ 0.25 .

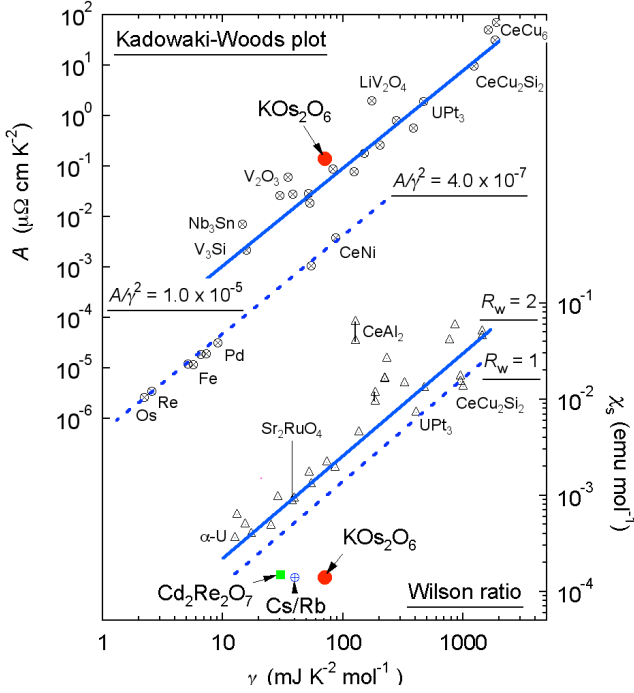


Fig. 7. Kadowaki-Woods plot and the Wilson ratio.

3.6. Superconductivity

The chemical trend of T_c is now discussed in the framework of conventional BCS theory. T_c is plotted as a function of the lattice constant a in Fig. 8(a). As the lattice is compressed by the chemical pressure, the T_c increases steeply toward K. This tendency is not compatible with a simple argument on a single-band model. However, it may not be surprising from the multi-band nature of these oxides. Saniz and Freeman discussed the trend of T_c and estimated T_c based on the McMillan-Allen-Dynes formalism [16]. They claimed that the incorporation of an electron-spin coupling is required to reproduce the experimental T_c .

We discuss in a simple way to deduce the relationship between T_c and DOS, using an equation

$$T_c = \omega_{\text{ph}} \exp\left(-\frac{1}{N(0)V}\right)$$

where ω_{ph} is a frequency of a relevant phonon, $N(0)$ the DOS at the Fermi level, and V the pairing potential. Let us assume that T_c depends only on the $N(0)$, keeping both the ω_{ph} and V constant over the compounds. Then, the T_c of one compound can be calculated from that of the other as

$$T_c' = \omega_{\text{ph}} \exp\left[\frac{N(0)}{N'(0)} \ln\left(\frac{T_c}{\omega_{\text{ph}}}\right)\right].$$

Provided $T_c = 1.0$ K and $\gamma = 30.2$ $\text{mJ K}^{-2} \text{ mol}^{-1}$ (γ is proportional to $N(0)$) for $\text{Cd}_2\text{Re}_2\text{O}_7$ as a reference, one can estimate T_c 's for the others for a certain phonon energy. Figure 8(b) depicts the results for $\omega_{\text{ph}} = 460$ K, which is the Debye temperature of $\text{Cd}_2\text{Re}_2\text{O}_7$ [2], 300 K, and 50 K. Apparently, the two high-energy phonons can reproduce T_c for Cs and Rb ($T_c' = 4.5$ K and 4.0 K for $\omega_{\text{ph}} = 460$ K and 300 K), while overestimate for K. On the other hand, the

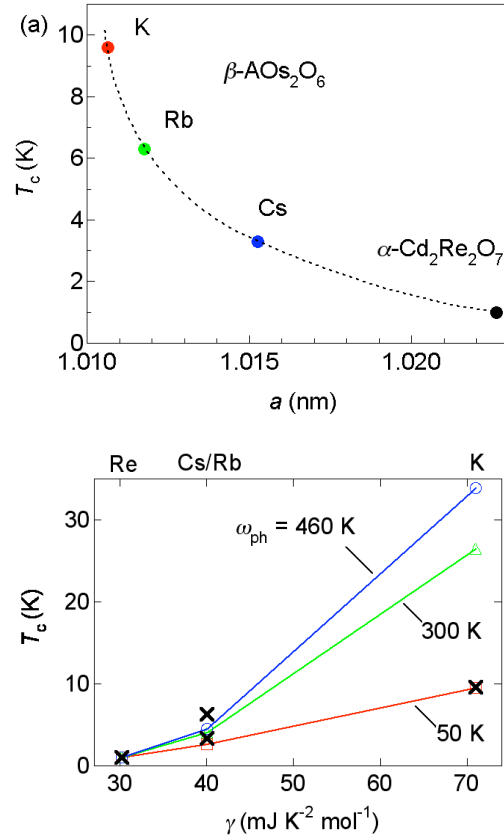


Fig. 8. (a) Variation of T_c with the lattice constant a for pyrochlore oxide superconductors. (b) Comparison of experimental and calculated T_c 's as a function of the Sommerfeld coefficient γ . Experimental T_c values are shown by crosses, and those calculated by open marks for 3 cases of different phonons; $\omega_{\text{ph}} = 460$ K, 300 K, and 50 K.

low-energy phonons of 50 K gives $T_c' = 2.6$ K for Cs/Rb and 9.5 K for K, in good agreement for K. Therefore, one identical phonon can not explain the change of T_c . It is plausible that a relevant phonon energy decreases for KOs_2O_6 , which suppress the increase of T_c due to the rise in the DOS.

The role of low energy phonons on the mechanism of superconductivity has been studied in many strong-coupling superconductors, such as Pb, A15 and Chevrel phase compounds. The correction for the BCS ratio, $\Delta C/\gamma T_c$, by the strong electron-phonon interactions was deduced in the following form [41];

$$\frac{\Delta C}{\gamma T_c} = 1.43 \left[1 + 53 \left(\frac{T_c}{\omega_{\text{log}}} \right)^2 \ln \left(\frac{\omega_{\text{log}}}{3T_c} \right) \right].$$

Using this equation, we estimate ω_{log} to be 59 K for KOs_2O_6 . Then, a coupling constant λ can be obtained from the McMillan-Allen-Dynes equation [42];

$$T_c = \frac{\omega_{\text{log}}}{1.2} \exp \left[\frac{-1.04(1 + \lambda)}{\lambda - \mu^*(1 + 0.62\lambda)} \right],$$

where μ^* is the Coulomb coupling constant and was calculated to be 0.096, 0.093, and 0.091 for Cs, Rb, and K, respectively [16]. The λ value for K is thus determined to be 2.38, which is much larger than that of typical strong-coupling superconductors like Pb ($\lambda = 1.55$, $\omega_{\text{log}} = 50$ K) and Mo_6Se_8 ($\lambda = 1.27$, $\omega_{\text{log}} = 70$ K) and is comparable with that of a Bi-Pb alloy ($\lambda = 2.1$, $\omega_{\text{log}} = 45$ K) [42]. Therefore, KOs_2O_6 is an extremely strong-coupling superconductor.

It is reasonable to ascribe such a low-energy phonon to the rattling vibration in the case of the β pyrochlores. The observed unusual enhancements of γ or H_{c2} toward K must be related to the lowering of the characteristic energy of the rattling, as shown in Fig. 4. It would be an intriguing question how this rattling, which is an essentially anharmonic vibration almost localized in a cage, can mediate Cooper pairing in KOs_2O_6 .

3.7. Pressure dependence of T_c

Pressure effects on T_c for the β pyrochlores have been studied experimentally [26, 29, 43] and theoretically [16]. As expected from the dependence of T_c on the lattice constant shown in Fig. 8(a), the T_c initially increases with compressing the lattice by applying physical pressure. Then, it reaches a maximum value, gradually decreases with further increasing pressure, and is finally suppressed above a critical pressure [26]. Although the maximum value and the critical pressure depend on the A elements, a bell-shaped T_c variation is commonly observed. Saniz and Freeman evaluated the pressure effects quantitatively and found that pressure effects on the overall electronic

structures are rather small [16]. It was found, however, that T_c increases with pressure in spite that both the DOS and λ_{ep} decrease with pressure. This is mainly because μ^* as well as μ_{ep} (the electron-spin coupling constant), which are effective to reduce T_c , decrease more rapidly.

In order to get more insights on what happens under high pressure, we carried out structural study under high pressure up to 7 GPa and obtained volume compressibility for all the members of β pyrochlores. It is almost linear with pressure for Rb and K and tends to saturate for Cs. By fitting the data to the form, $\Delta V/V_0 = -\alpha P + \beta P^2$, we obtained that $\alpha = 0.00726$ (GPa) $^{-1}$ for K, $\alpha = 0.00777$ (GPa) $^{-1}$ for Rb, and $\alpha = 0.00756$ (GPa) $^{-1}$ and $\beta = 0.000198$ (GPa) $^{-2}$ for Cs. Using these values, the pressure dependence of T_c reported in Ref. 26 is transformed to a volume dependence of T_c as shown in Fig. 9. Interestingly, the three sets of data merge into a single straight line at low volume. Deviation from this universal line occurs at a different volume that increases from Cs to K. It seems that K takes the highest T_c due to the fact that it keeps the universal line up to the largest volume. The initial increase of T_c with volume may be attributed to the increase of DOS according to the bandstructure calculations. On the other hand, the decrease of T_c above the maximum may be related to the decrease in the energy of relevant phonons. Further investigations are required to understand these features.

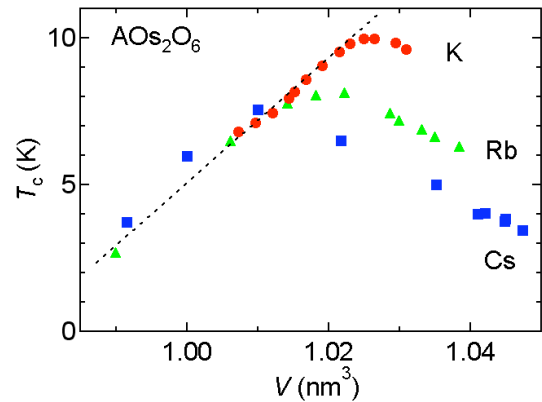


Fig. 9. Cell volume dependence of T_c .

4. Concluding remarks

Finally, we add 4 points for the pyrochlore oxide superconductors to the well-known T_c - γ diagram shown in Fig. 10. The β -pyrochlores, especially KOs_2O_6 , exist close to the Chevrel phase family in the map, and are characterized as a new member of strong-coupling superconductors. It is suggested in the β pyrochlores, as in other strong-coupling superconductors, that low-energy phonons play a crucial role in the pairing mechanism, and that it comes from the rattling of the alkali metal ions. We think that future systematic study on the pyrochlore

superconductors would extend the horizon for understanding the physics of strong-coupling superconductivity.

Acknowledgments

We thank M. Takigawa and Y. Matsuda for enlightening discussions, and N. Takeshita and his coworkers for providing unpublished high-pressure data on a single crystal of KOs_2O_6 . This research was supported by a Grant-in-Aid for Scientific Research B (16340101) provided by the Ministry of Education, Culture, Sports, Science and Technology, Japan.

References

- [1] J. G. Bednorz, K. A. Müller, *Z. Phys. B* 64 (1986) 189.
- [2] M. Hanawa, Y. Muraoka, T. Tayama, T. Sakakibara, J. Yamaura, Z. Hiroi, *Phys. Rev. Lett.* 87 (2001) 187001.
- [3] S. Yonezawa, Y. Muraoka, Z. Hiroi, *J. Phys. Soc. Jpn.* 73 (2004) 1655.
- [4] S. Yonezawa, Y. Muraoka, Y. Matsushita, Z. Hiroi, *J. Phys. Soc. Jpn.* 73 (2004) 819.
- [5] S. M. Kazakov, N. D. Zhigadlo, M. Brühwiler, B. Batlogg, J. Karpinski, *Supercond. Sci. Technol.* 17 (2004) 1169.
- [6] M. Brühwiler, S. M. Kazakov, N. D. Zhigadlo, J. Karpinski, B. Batlogg, *Phys. Rev. B* 70 (2004) 020503R.
- [7] S. Yonezawa, Y. Muraoka, Y. Matsushita, Z. Hiroi, *J. Phys.: Condens. Matter* 16 (2004) L9.
- [8] On KOs_2O_6 , Yamaura *et al.* reported the space group $Fd-3m$ [*J. Solid State Chem.* 179 (2005) 336], while, recently, Schuck *et al.* claimed a different space group of $F-43m$ without inversion symmetry at room temperature [*Phys. Rev. B* 73 (2006) 144506]. We carefully reexamined the crystal structure using a high-quality crystal and found that $Fd-3m$ is the most probable space group for KOs_2O_6 , in spite that we observed some forbidden reflections due to double reflections.
- [9] S. Yonezawa, T. Kakiuchi, H. Sawa, J. Yamaura, Y. Muraoka, F. Sakai, Z. Hiroi, submitted to *Solid State Sciences*.
- [10] J. Yamaura, S. Yonezawa, Y. Muraoka, Z. Hiroi, *J. Solid State Chem.* 179 (2005) 336.
- [11] Z. Hiroi, S. Yonezawa, T. Muramatsu, J. Yamaura, Y. Muraoka, *J. Phys. Soc. Jpn.* 74 (2005) 1255.
- [12] J. Kunes, T. Jeong, W. E. Pickett, *Phys. Rev. B* 70 (2004) 174510.
- [13] H. Harima, *J. Phys. Chem. Solids* 63 (2002) 1035.
- [14] D. J. Singh, P. Blaha, K. Schwarz, J. O. Sofo, *Phys. Rev. B* 65 (2002) 155109.
- [15] R. Saniz, J. E. Medvedeva, L. H. Ye, T. Shishidou, A. J. Freeman, *Phys. Rev. B* 70 (2004) 100505.
- [16] R. Saniz, A. J. Freeman, *Phys. Rev. B* 72 (2005) 024522.
- [17] A. W. Sleight, J. L. Gillson, J. F. Weiher, W. Bindloss, *Solid State Commun* 14 (1974) 357.
- [18] D. Mandrus, J. R. Thompson, R. Gaal, L. Forro, J. C. Bryan, B. C. Chakoumakos, L. M. Woods, B. C. Sales, R. S. Fishman, V. Keppens, *Phys. Rev. B* 63 (2001) 195104.
- [19] Z. Hiroi, M. Hanawa, *J. Phys. Chem. Solids* 63 (2002) 1021.
- [20] O. Vyaselev, K. Kobayashi, K. Arai, J. Yamazaki, K. Kodama, M. Takigawa, M. Hanawa, Z. Hiroi, *J. Phys. Chem. Solids* 63 (2002) 1031.
- [21] Z. Hiroi, S. Yonezawa, J. Yamaura, T. Muramatsu, Y. Muraoka, *J. Phys. Soc. Jpn.* 74 (2005) 1682.
- [22] Z. Hiroi, S. Yonezawa, J. Yamaura, Y. Muraoka, submitted to *J. Phys.: Condens. Matter*; cond-mat/0607064.
- [23] Z. Hiroi, S. Yonezawa, *J. Phys. Soc. Jpn.* 75 (2006) 043701.
- [24] K. Arai, J. Kikuchi, K. Kodama, M. Takigawa, S. Yonezawa, Y. Muraoka, Z. Hiroi, *Physica B* 359-361 (2005) 488.
- [25] E. Ohmichi, T. Osada, S. Yonezawa, Y. Muraoka, Z. Hiroi, *J. Phys. Soc. Jpn.* 75 (2006) 045002.
- [26] T. Muramatsu, N. Takeshita, C. Terakura, H. Takagi, Y. Tokura, S. Yonezawa, Y. Muraoka, Z. Hiroi, *Phys. Rev. Lett.* 95 (2005) 167004.
- [27] A. Koda, W. Higemoto, K. Ohishi, S. R. Saha, R. Kadono, S. Yonezawa, Y. Muraoka, Z. Hiroi, *J. Phys. Soc. Jpn.* 74 (2005) 1678.
- [28] K. Magishi, S. Matsumoto, Y. Kitaoka, K. Ishida, K. Asayama, M. Uehara, T. Nagata, J. Akimitsu, *Phys. Rev. B* 57 (1998) 11533.
- [29] R. Khasanov, D. G. Eshchenko, J. Karpinski, S. M. Kazakov, N. D. Zhigadlo, R. Brutsch, D. Gavillet, D. D. Castro, A. Shengelaya, F. L. Mattina, A. Maisuradze, C. Baines, H. Keller, *Phys. Rev. Lett.* 93 (2004) 157004.
- [30] R. Khasanov, D. G. Eshchenko, D. D. Castro, A. Shengelaya, F. L. Mattina, A. Maisuradze, C. Baines, H. Luetkens, J. Karpinski, S. M. Kazakov, H. Keller, *Phys. Rev. B* 72 (2005) 104504.
- [31] T. Schneider, R. Khasanov, H. Keller, *Phys. Rev. Lett.* 94 (2005) 077002.
- [32] M. Brühwiler, S. M. Kazakov, J. Karpinski, B. Batlogg, *Phys. Rev. B* 73 (2006) 094518.
- [33] G. Schuck, S. M. Kazakov, K. Rogacki, N. D. Zhigadlo, J. Karpinski, *Phys. Rev. B* 73 (2006) 144506.
- [34] Y. Kasahara, Y. Shimono, T. Shibauchi, Y. Matsuda, S. Yonezawa, Y. Muraoka, Z. Hiroi, *Phys. Rev. Lett.* 96 (2006) 247004.
- [35] Z. Hiroi, in preparation.
- [36] A. P. Mackenzie, R. K. Haselwimmer, A. W. Tyler, G. G. Lonzarich, Y. Mori, S. Nishizaki, Y. Maeno, *Phys. Rev. Lett.* 80 (1998) 161.
- [37] K. Kuroki, Y. Tanaka, R. Arita, *Phys. Rev. Lett.* 93 (2004) 077001.
- [38] K. Kadowaki, S. B. Woods, *Solid State Commun* 58 (1986) 507.
- [39] K. Miyake, T. Matsuura, M. Varma, *Solid State Commun* 71 (1989) 1149.
- [40] O. Vyaselev, K. Arai, K. Kobayashi, J. Yamazaki, K. Kodama, M. Takigawa, M. Hanawa, Z. Hiroi, *Phys. Rev. Lett.* 89 (2002) 017001.
- [41] F. Marsiglio, J. P. Carbotte, *Phys. Rev. B* 33 (1986) 6141.
- [42] P. B. Allen, R. C. Dynes, *Phys. Rev. B* 12 (1975) 905.
- [43] T. Muramatsu, S. Yonezawa, Y. Muraoka, Z. Hiroi, *J. Phys. Soc. Jpn.* 73 (2004) 2912.

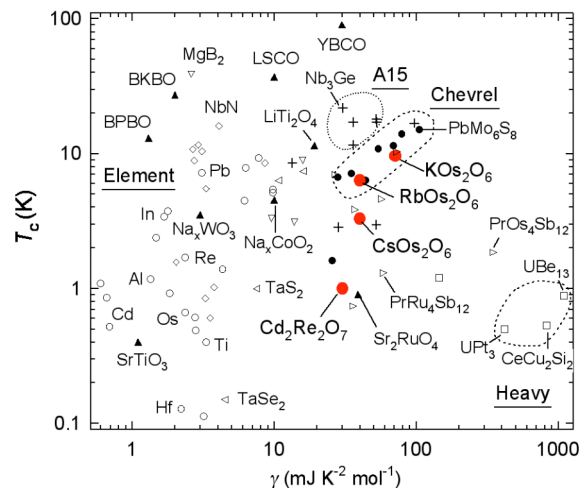


Fig. 10. Various superconductors mapped in the T_c - γ diagram.